Tethys, 6, 51–66, 2009
Journal of Weather & Climate of the Western Mediterranean
www.tethys.cat
ISSN-1697-1523
eISSN-1139-3394
DOI:10.3369/tethys.2009.6.04

Journal edited by **ACAM**
(Associació Catalana de Meteorologia)

Shallow convection over land: a mesoscale modelling study based on idealized WRF experiments

J. T. M. Lenaerts[1], **C. C. van Heerwaarden**[1] **and J. Vilà-Guerau de Arellano**[1]

[1]Meteorology and Air Quality Section, Wageningen University and Research Center, The Netherlands

Received: 16-X-2008 – Accepted: 10-III-2009 – **Original version**

Correspondence to: J.Lenaerts@uu.nl

Abstract

A shallow cumulus over land redistributes heat and moisture in the boundary layer, but is also important on larger scales, because it can trigger severe convection events. Due to its small (10^2 - 10^3 m) spatial scale, this feature is defined as a sub-grid process in mesoscale models. The goal of this research is to examine the representation of shallow cumulus clouds in the mesoscale model WRF by reproducing a shallow cumulus situation observed over land. In particular, we focus on the role of the convection parameterisation in the characteristic vertical energy transport in the boundary layer. The analysis focusses on the thermodynamic structure of the boundary layer and on the cloud properties derived from a simple parcel method theory. This numerical experiment is designed to be as close as possible to the Large-Eddy Simulations (LES) model intercomparison study of Brown et al. (2002). They concentrated on the representation of shallow cumulus clouds over land in LES, using data from the American Southern Great Plains of 21st June 1997. To imitate the dynamic structure of LES, we have designed a Multiple Single Column version of WRF. Using identical surface forcing and initial thermodynamic profiles, WRF boundary layer structure shows good agreement with the LES results. However, the parcel method indicates that a larger inversion and the absence of a conditionally unstable layer suppress shallow cumulus clouds development by WRF. In addition, WRF does not show any cloud development in terms of cloud liquid water. We show also that a convective parameterisation is necessary to represent the enhanced boundary layer vertical transport by shallow cumulus clouds. Different convective parameterisation schemes are analyzed and compared.

Key words: Shallow cumulus, mesoscale modelling, WRF - parameterisation

1 Introduction

Shallow cumulus clouds are not only important for the boundary layer structure, as they redistribute heat and moisture vertically within, but they can also initiate severe convection in regions over land (Lenderink et al., 2004; hereafter LE04). In the Mediterranean region all summertime precipitation is associated with convective instability (Tudurí and Ramis, 1997). At a global scale, shallow cumulus convection forms a substantial part of the Hadley circulation, initiating deep convection in the tropics (Tiedtke, 1989).

However, shallow cumuli are characterised by spatial scales smaller than 1 km and therefore their representation in present large and mesoscale circulation models, used for climate research or operational purpose, is relatively poor (LE04). For a correct representation of vertical transports of heat and momentum in typical boundary layer circulations, a resolution of 4 km or smaller is needed (Kuo et al., 1997), which is a degree of detail in practice that is rarely used. Typical boundary layer phenomena like shallow cumulus have a length scale which is smaller than the typical grid size of a mesoscale model and are, therefore, referred to as sub-grid scale processes. These processes are not resolved on this grid size and need to be parameterised. However, mesoscale models with high horizontal and vertical resolution and explicit physical parameterisation have become powerful tools

in research and operational modelling (Kuo et al., 1997); in that respect, Petch et al. (2002) conclude that the horizontal resolution should be no coarser than one fourth of the subcloud layer depth (100 - 500 m) to explicitly resolve the key processes connected to shallow convection, which is computationally expensive. Therefore, considerable efforts have been made to improve shallow cumulus parameterisations in models (Tiedtke, 1989, Kain, 2004, Zhu and Bretherton, 2004, Neggers et al., 2007, de Rooy and Siebesma, 2008), but still, the typical interaction between subcloud and cloud layer is poorly understood (Neggers et al., 2004). Using theoretical and observational analysis such as the mixed layer model (Zhu and Albrecht, 2002) or a Large-Eddy Simulation (LES) model (Brown et al., 2002; hereafter BR02, Siebesma et al., 2003), research has been done on the onset and formation of shallow cumulus clouds over land. Others compared the performance of a set of Single Column Models (SCM) to represent cumulus clouds (LE04).

More recently, specific model studies have focussed to increase the understanding about the physics and dynamics of shallow cumulus over land (Zhu and Albrecht, 2002; BR02; Ek and Holtslag, 2004; LE04; Vilà-Guerau de Arellano, 2007). In contrast to shallow cumuli over the sea, this process is largely dependent on strong, time varying surface fluxes. The unsteadiness of the problem case could make it difficult to model (BR02). In this respect, Large-Eddy Simulations can provide detailed diagnostics and allow sensitivity analysis of individual variables. BR02 evaluated the reliability of 8 independent LES models simulating shallow cumuli over land. This intercomparison has shown great consistency with observations and within the models, and has therefore proven to be a valuable reference dataset. Furthermore, LE04 have studied the performance of a set of semi-operational Single-Column Models. In particular, they emphasised the behaviour of different cumulus parameterisation schemes (CPS) involved. Results show a wide scatter, which suggests that there is further need for knowledge about the development and improvement of parameterisation schemes, particularly in the case of unsteady boundary layer development. Both studies are based on an idealisation of observations made at the Southern Great Plains (SGP) measurement facility, Oklahoma, USA, during the Atmospheric Radiation Measurement (ARM) on 21st June 1997. On this particular day, shallow cumulus clouds developed at the top of a convective boundary layer (BR02).

LES models (BR02) are set up to explicitly calculate small-scale processes in the atmosphere. Mesoscale models, like WRF, however, have larger grid lengths and represent turbulent motions by solving Reynolds-averaged equations. Subgrid processes have to be parameterised. Up to now, little attention has been paid to the performance of a full 3D mesoscale model to model shallow cumuli over land and the role of the CPS in this. In our opinion, this is an essential step in the process of improving parameterisation schemes. In order to investigate it, we select and adapt the mesoscale model WRF (Skamarock et al., 2005) to carry out a similar numerical experiment as BR02. Our methodology is based on a 3D grid raster of identical vertical columns, which can be interpreted as Multiple Single Columns (MSC), which interact among each other permitting horizontal advection, unlike the Single-Column Model methodology. Applying the MSC strategy removes all horizontal land surface heterogeneities, which can influence convection patterns significantly (e.g. van Heerwaarden and Vilà-Guerau de Arellano, 2008). It is important to mention that the numerical experiment is designed to be as close as possible to the LES study from BR02.

The first objective of this study is to evaluate the representation of shallow cumulus clouds over land by WRF. Our approach focuses on the analysis of thermodynamic profiles using the parcel method, with special emphasis on atmospheric stability and inversion strength and evolution of important cloud properties. We use the results of BR02 to evaluate our WRF results. Secondly, depending on these results, we will discuss the performance of the cumulus parameterisation scheme in a mesoscale model, since shallow cumuli are dependent on the cumulus parameterisation. In particular we emphasise the role of a CPS in the sub-grid vertical transport of heat and moisture within the shallow cumulus boundary layer. Therefore, WRF simulations with and without CPS are analysed and compared. The Kain-Fritsch CPS (Kain and Fritsch, 1990; hereafter KF) has recently been updated with a new shallow cumulus sub-scheme (Kain, 2004). For this reason this scheme will be used in our study, but its performance will also be evaluated against the Grell CPS (Grell, 1993). The choice of the CPS can greatly affect the resulting convective behaviour of the model, like the location and intensity of convective rainfall patterns in the western Mediterranean (Buzzi et al., 1994, Callado and Pascual, 2005).

The outline of this paper is as follows. In Section 2, we will explain the methodology that we have used in this study; we will elaborate further on the concept of MSC and control experiment, specify the numerical details and give a short introduction to the parameterisation schemes. In Section 3, the results will be shown. Conclusions and remarks can be found in Section 4.

2 Methodology

2.1 Selected meteorological situation

The case is based on observational data of the SGP ARM measurement site on 21st June 1997. For this study we will only use the data obtained at the Central Facility (N 36°36', W 97°29'). Due to the large amount of available data and the homogeneity and flatness of the land surface, this site is extremely well suited for this study. Besides, the day of 21st June 1997 shows ideal conditions for shallow cumulus cloud formation. During the morning the surface fluxes increased to a maximum around noon, and as a result a convective boundary layer developed. Wind direction did not change in height or time (BR02). As a result, observa-

tions show the formation of shallow cumulus clouds in the morning, which persisted during the afternoon and slowly died down at dawn. Cloud cover data indicate that it did not exceed 50%. Based on these findings, a LES intercomparison study was set up (BR02). A great amount of model input that has been described in this study will be re-used here, in order to obtain a valid comparison.

2.2 Control Experiment

Our goal is to reproduce the above-described case by means of a control experiment. We have chosen the mesoscale model WRF (Skamarock et al., 2005), which is widely used for research and operational goals. In the Mediterranean, WRF is used, among others, to model air quality in Catalunya (Jimenez-Guerrero et al., 2008) and for climate predictions (Hahmann et al., 2008). This model can be representative for the ability of mesoscale models to reproduce the sub-grid scale shallow convection over land and microphysics involved. Below, we will focus briefly on the characteristics of the WRF model. We have used version 2.2 of the WRF-ARW solver. In normal (operational) configuration, a mesoscale model like WRF should be provided with initial and boundary conditions from a global model. In the current configuration, however, we have chosen to run WRF with periodic boundary conditions in horizontal directions, similar to LES simulations. Although periodic boundary conditions prevent us from modelling real-world boundary layers (Moeng, 2006), this technique could be valuable in evaluating the capacity of WRF to reproduce the shallow cumulus cloud effects and to determine the potential influence of surface heterogeneity on cloud formation. Furthermore, the same initial thermodynamic profiles and wind speed are prescribed at each grid cell in all the domains.

We used 3 domains, with the largest domain of size at 656 x 656 km^2 (41 grid cells of 16 km grid length), the second domain is 164 x 164 km^2 (41 grid cells of 4 km grid length) and the third from about 41 x 41 km^2 (41 grid cells of 1 km grid length). In each domain we used 60 vertical levels, of which 30 were defined in the boundary layer, to insure sufficient vertical resolution. The second and third domain are one-way nested with their parent domain. The domains are centred on the ARM Central Site. Figure 1 shows the set up of the WRF numerical experiment, defining three domains with identical initialisation of the vertical thermodynamic profiles.

The model is run from 21st June 11 UTC (6 LT = 6 Local Time = UTC - 5 hours) until 21st June 23 UTC (18 LT) to reproduce the daily evolution. Results are stored every full hour. It is important to mention that all the results presented here are spatially averaged within the third domain. In this respect, we assume that due to the homogeneity of the domains, the spatially averaged data is identical to the data of the centred grid point. Note that also BR02 (domain 6.4 x 6.4 km^2) made the same assumption, and according to their results, it is justified to use this assumption due to the homogeneity of the land surface.

The initial profiles (6 LT) of potential temperature and specific humidity, which are prescribed for every grid cell in all the domains, are shown in Figure 1. These profiles were suggested by BR02, based on the ARM observations. They were also used by LE04. We refer to B02 for more details about the construction of the initial profiles. Note that the sun appears around 6:10 LT on that day. In short, one can distinguish 4 specific regions in this profile: (a) a very shallow morning stable surface layer; (b) an early morning boundary layer (up to 800 m); (c) a conditionally unstable region allowing the CBL (Convective Boundary Layer) to grow during the day (800 - 2700 m) and (d) a stable region representing the troposphere (2700 - 5500 m). It should be noted that, in contrast with LES, the WRF model consists of vertical air columns, which extend up to the troposphere, which is about 16 km above the ground in this case. While the LES initial profiles are prescribed up to 5.5 km (BR02), we have to extrapolate the profiles vertically; a constant potential temperature decrease between 5.5 and 16.5 km height of 3.772 K km^{-1} and a linearly decreasing mixing ratio from 3 to 0 g kg^{-1} from 3 to 5.5 km and a zero mixing ratio above that height has been applied. Similar to BR02, we have initiated the simulation with a wind of U = (10,0). The roughness length has been fixed to the value suggested by BR02, which led to an improvement of the surface flux values compared to the case with a default roughness length.

In BR02 the surface turbulent fluxes are prescribed during the whole simulation. In our study, we decide to allow the surface flux to be coupled with the atmospheric condition, but to adjust it as close as possible to the surface forcings used in BR02. A detailed description of the surface scheme can be found in Braun and Tao (2000) (Appendix B) and Steeneveld et al. (2008). Therefore, we have modified some surface parameters of the sensible and latent heat flux. In Table 1, the values of these prescribed parameters are given. Soil moisture is an important parameter, because it is directly used in the surface parameterisation to calculate the latent heat flux.

In our experiments, skin temperature has been decreased compared to the reference value, because the morning values of the sensible heat flux showed large negative values, even after sunrise, which is intuitively not realistic. Apparently, with a default skin temperature, the problem raised that in the early morning hours, with a small initial difference between skin and air temperature, the air temperature already started to increase, while the skin temperature remained constant. As a consequence, the temperature difference became too low, and so did the sensible heat flux.

The soil temperatures are therefore adjusted in order to insure a realistic initial flux partition. The first layer is 1 K warmer than skin temperature, so the soil heat flux is directed upwards before sunrise. The temperature evolution shows a realistic behaviour: skin temperature extends to the first ground temperature at 7:30 LT -corresponding to a

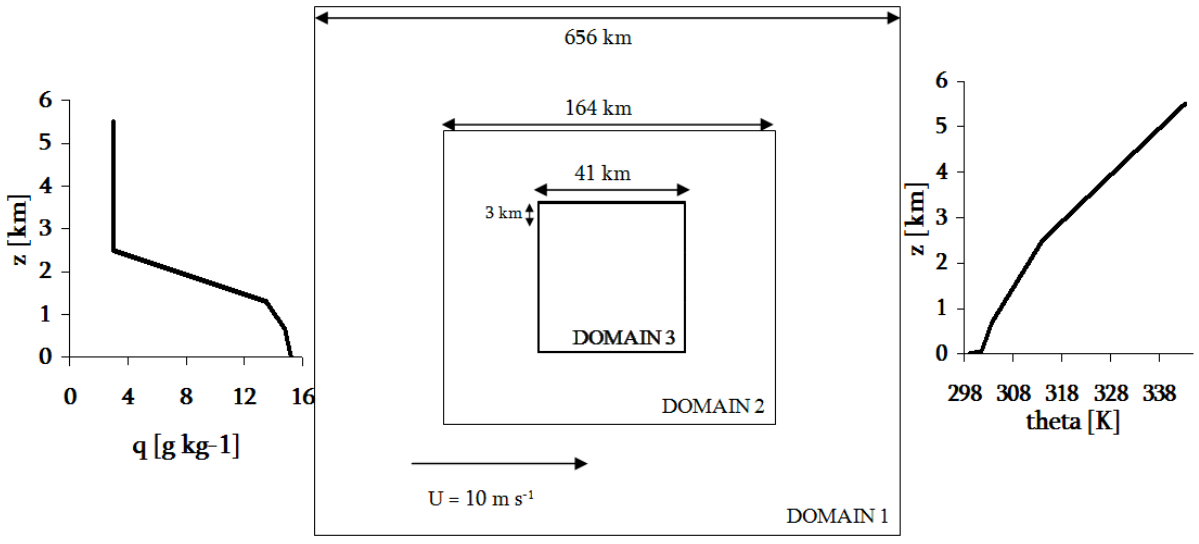

Figure 1. Sketch of the numerical set-up in the mesoscale model WRF (not to scale). The initial profiles of specific humidity (left) and potential temperature (right) and wind speed are also shown.

positive sensible heat flux, which is about 1.5 hour after sunrise.

Large-scale advective fluxes were relatively small compared to the local surface forcing, and LES model tests proved that these terms have only a minor impact on the simulations (BR02). Therefore, no large-scale fluxes are prescribed in our simulations.

In this study, we focus on modelling shallow convection with a mesoscale model. In this respect, the problem arises that a shallow cumulus has a typical length scale which is smaller than the grid size from the model. In other words, shallow cumulus is called a sub-grid scale feature. This means that effects of shallow convection is not represented by the model and it is required to use a parameterisation to account for the transport driven by shallow cumulus convection.

Earlier work has demonstrated the advantage of a CPS that directly calculates moist convective updrafts, in particular Kain-Fritsch and Grell (Wang and Seaman, 1997). The scheme developed by Grell (Grell, 1993; Grell et al., 1995) is currently considered by the mesoscale modelling community as a scheme that performs well with typical grid sizes of a few kilometres (Kuo et al., 1997). The recently updated scheme is using an ensemble technique that is used in WRF (Grell and Devenyi, 2002). On the other hand, previous studies show positive results with KF CPS, comparing different parameterisations (Gochis et al., 2002); others report that KF provided a very realistic representation of sub-grid-scale moist convection, studying intense Atlantic cyclones (Kuo et al., 1996); another study concluded the KF scheme to be the most robust simulating six different cases on the US continent (Wang and Seaman, 1997). However, it remains unclear which physical mechanisms cause the KF scheme to outperform other schemes in these cases. Liang et al. (2004) studied the diurnal evolution of precipitation in the USA, using KF and Grell in the MM5 model. They concluded that both schemes have their strong and weak points, but no scheme outperformed the other. Differences were attributed to the fact that KF is responsive to boundary layer forcing, while Grell is more reactive to large-scale tropospheric forcing (Liang et al., 2004). Furthermore, as described in detail below, the new KF-ETA version (Kain, 2004) includes a particular shallow convection sub-scheme. For these reasons, we have chosen to focus on the KF parameterisation scheme in this study. In order to justify this choice, we have included a short comparison between Grell and KF in the results.

The Kain-Fritsch scheme, which is used in this study, has been derived from the original Fritsch-Chappell scheme (Fritsch and Chappell, 1980). Until now, it has been updated and improved several times (Kain and Fritsch, 1990 and 1992). The latest version, which is included in the WRF model code, has been successfully tested in the ETA model (Kain, 2004). This version contains a new shallow cumulus convection scheme. Briefly, the KF CPS is a mass flux scheme, which includes updraft and downdraft calculations. It uses the Langragian parcel method, which determines on which vertical model levels instability exists, if that layer would be available for cloud growth (updraft source layer), and, if so, which type of cloud then satisfies the ambient conditions (Kain, 2004).

As mentioned, in the KF-ETA version (Kain, 2004), a new parameterisation for shallow cumulus convection has been implemented. Shallow convection is activated only if all conditions for deep convection have been satisfied, except

Table 1. Surface parameters prescribed in the WRF simulations to reproduce the surface forcing of BR02.

Variable/parameter	Units	Value
Fixed parameters		
Albedo	-	18%
Soil moisture availability	-	48%
Roughness Length	m	0.035
Thermal Inertia	cal cm^{-2} k^{-1} $s^{-1/2}$	4
Surface heat capacity per unit volume	J m^{-3} K^{-1}	25 $.10^5$
Variable parameters		
Surface Pressure	Pa	100562.9
Skin Temperature	K	297
Ground Temperatures	K	Depth = 1 cm: 298
		2 cm: 298.1
		4 cm: 298.3
		8 cm: 298.7
		16 cm: 293.3

that the minimal cloud depth is not exceeded. This cloud depth varies as a linear function of the temperature of the lifting condensation level (between 2 - 4 km). The deepest "shallow" cloud layer (with cloud depth>0) is then activated. In contrast with deep convection, the final updraft calculations mass flux decay is set linearly to the decreasing pressure within the cloud layer; at least this is qualitatively comparable to earlier LES results (Kain, 2004). The shallow cumulus clouds are also modulated by a different closure assumption. The cloud base mass flux M_{u0} is assumed to be a function of Turbulent Kinetic Energy (TKE). The subcloud maximum value of TKE_{max} (typically less than 10 m^2 s^{-2}) is used to quantify this mass flux.

2.3 Methods to analyze the model results

Before discussing the results, the main variables and methods used to analyse the results must be defined. In this study, we focus on the analysis of the structure of the vertical thermodynamic profiles, to discuss if, from a point of view of thermodynamic theory, clouds can potentially form. Moreover, we discuss the temporal evolution of these clouds, with emphasis on important level identification and cloud liquid water. In this respect, we define four important conditions for the formation of shallow cumulus (Vilà-Guerau de Arellano, 2007): (a) a lifting condensation level below the inversion; (b) absence of a temperature jump at the inversion; (c) a conditionally unstable temperature slope and (d) the possibility for a potential cloud to grow vertically up to the limit of convection. Note that these conditions are also used to define the initial potential temperature profile (BR02). Our analysis is based on determining the vertical structure of the profiles of θ_v and q_T in relation to the conditions mentioned above.

In the analysis we will emphasise the strength of the inversion and identification of stability regimes within the boundary layer, related to the conditions above. Below, we describe briefly the analysis applied to calculate the stratification stability of the thermodynamic profiles. Our analysis is based on the parcel method: a parcel is released at the surface and follows a theoretical vertical profile. By comparing the adiabatic profile of the parcel with the ambient profile, we can identify the stability of each different part of the boundary layer. Well-known relations describe the dry and moist adiabatic profiles. See e.g. Stull (2000) for definitions and more details.

In order to insure the formation and vertical development of clouds (see condition (d)) it is necessary that, in the cloud layer, the parcel remain warmer than its environment as it rises. Therefore, a conditionally unstable layer should be present (condition (c)), i.e. a layer with a temperature lapse rate which is not higher than the moist adiabat (stable). If the ambient lapse rate is stable, convection will be damped.

The analysis also focuses on the identification of important levels that define the depth of the cloud layer. For air at a pressure P, the saturation level is found by dry adiabatic ascent of an unsaturated air parcel, to the pressure level, P_{sp}, where the parcel is just saturated with no cloud liquid water (Stull, 1988). This level is also known as the lifting condensation level (LCL). In the profiles, the LCL is the boundary between the unsaturated regime (the subcloud layer) and the saturated regime (the cloud layer). The height of the LCL can be calculated in different ways; in this study we are using the empirical formula developed by Bolton (Bolton, 1980):

$$R_{LCL} = \frac{1}{\frac{1}{T_d - 56} + \frac{\ln \frac{T}{T_d}}{800}} + 56 \qquad (1)$$

in which T and T_d are the absolute and dew point temperatures (°C), respectively, at the first model vertical level. Because the air remains unsaturated, and therefore follows an unsaturated adiabat, we can make use of the integrated form of Equation 1 to obtain the height of the LCL. This height identifies the position of the LCL. Consequently, we can evaluate condition (a) by comparing the LCL height and the boundary layer height Z_i. Moreover, the height of the

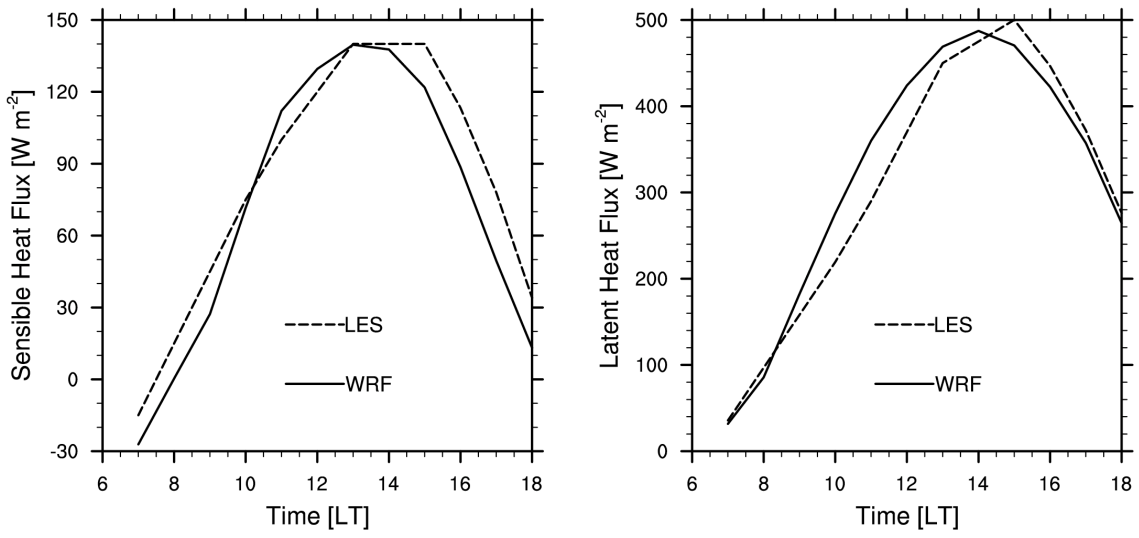

Figure 2. WRF modelled and prescribed surface fluxes on 21st June 1997. The modelled fluxes (averaged over the smallest domain) are shown in full lines. The dashed lines represent the prescribed surface forcings, which are fitted through observational flux values (BR02). The values at 6 LT are not shown, because they are absent in LES and zero in WRF.

LCL is the height where condensation starts; therefore we will use the LCL height as cloud base.

Besides the analysis of the thermodynamic characteristics of the convective boundary layer, it is helpful to determine the possible occurrence of clouds and analyse their properties. Therefore we will estimate the cloud base, cloud top and depth and compare the WRF with the LES results. In addition, the convective available potential energy (CAPE) is an appropriate variable to define the energy of a cloud layer, as it is a measure of the intensity of vertical motion of individual air parcels. Moreover, CAPE is used as the variable to close the mass flux scheme in Kain-Fritsch, as discussed before.

3 Results

3.1 Evaluation of surface turbulent fluxes

The formation of shallow cumulus over land is strongly dependent on the diurnal evolution of surface turbulent fluxes. In this respect, our goal was to obtain similar fluxes in WRF compared to LES. Figure 2 shows the sensible heat flux and the latent heat flux calculated by WRF and prescribed by LES. Notice that the WRF surface fluxes are calculated accounting for a land-atmosphere interaction. As mentioned, surface parameters were adjusted in order to obtain similar surface turbulent fluxes. Note that the surface layer is characterised by a friction velocity, related to the roughness length, which has been prescribed in the simulations with a similar value as in BR02 (see Table 1). The sensible heat flux maximum approximates 140 W m^{-2} and the latent heat flux maximum is approximately 490 W m^{-2}, which are both very comparable to the prescribed LES fluxes.

3.2 Diurnal Boundary Layer Structure

Similar magnitude and diurnal evolution of the calculated surface turbulent fluxes in WRF with the LES results shown in the previous subsection allow us to extend the analysis by comparing the boundary layer structure evolution of WRF and LES during the day. Figure 3 shows the vertical profiles of θ_v and q_T of LES and WRF for three time steps: 11 LT, 14 LT, and 17 LT, in order to analyse the development, the peak activity and breakdown of the shallow cumulus during the day, respectively. Note that daylight is present from 6:10 LT and the sun sets around 20:50 LT. The dry and moist adiabatic profiles, which are constructed as described in the previous section, are also included. It is interesting to look at the difference between the analysis with the parcel method and the model results. Therefore, we have also added the cloud base and top calculated by LES.

The WRF results are averaged over all grid points within the (smallest) domain. Note that we did not include observational data in this analysis since we assume LES to be consistent with observations (BR02). LES data represent a more detailed temporarily and spatially averaged atmospheric state than observations.

At 11 LT, a well-mixed boundary layer has developed with a bulk temperature of about 305.5 K for WRF and about 306 K for LES. The mixed layer total specific humidity is around 16 g kg^{-1} for both models; LES is slightly drier than WRF. The mixed layer calculated by LES extends up to about 800 m, while the WRF profile shows a deeper mixed layer from about 1200 m. This difference can be caused by the fact that we used the Medium-Range Forecast (MRF; Hong and Pan, 1996) boundary layer scheme in WRF, which has

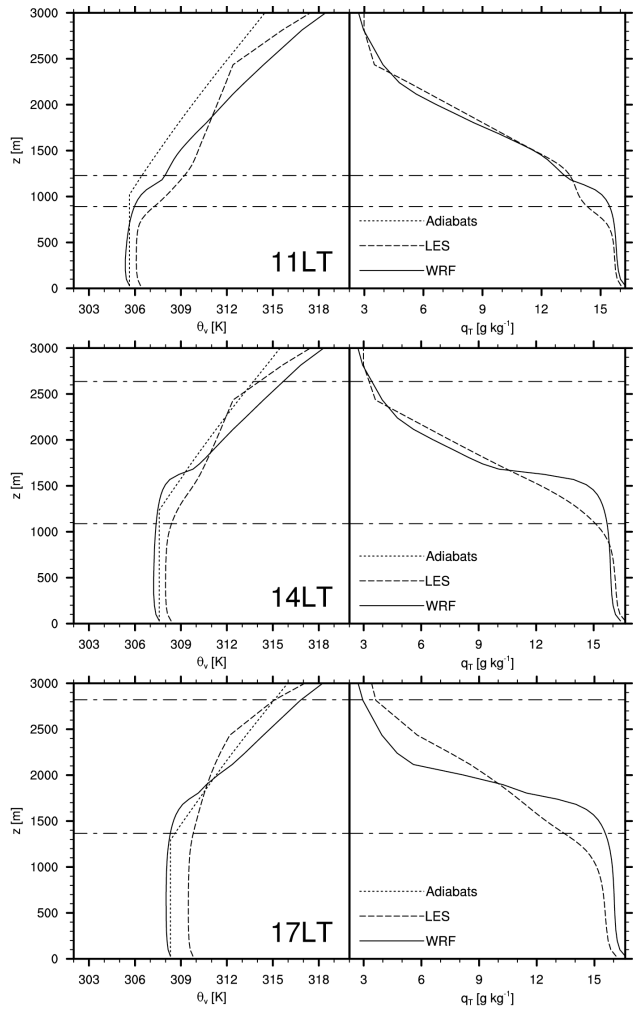

Figure 3. Vertical profiles of virtual potential temperature (θ_v, left) and total specific humidity (q_T, right) from WRF (full) and LES (dashed), for three time steps during 21st of June 1997: 11 LT (above), 14 LT (middle) and 17 LT (below). The dry and moist adiabats that belong to WRF profiles are also included (dotted). The horizontal lines represent the cloud base and top calculated by LES. They are defined as the lowest and uppermost level at which $q_L > 0$, respectively.

a tendency to overestimate boundary layer growth (Zhong et al., 2007). A sensitivity test using the Eta-Mellor-Yamada (ETA; Janjić, 1994) boundary layer scheme did show some better results regarding the determination of boundary layer height, because it creates a shallower boundary layer, but also showed a large bias in mixed layer temperature and humidity. Analysing the LES results, if we focus on the region above the boundary layer, we find the smaller lapse rate in LES between the cloud top and 2500 m; this indicates a conditionally unstable tropospheric layer, which is a necessary condition for shallow cumulus growth further during daytime, as we mentioned in the previous section. The cloud can potentially develop to the level where this regime ends (about 2.5 km high), and even higher, when it loses all its positive buoyancy by overshooting into the stable region. Instead, WRF lapse rate is higher than the moist adiabat, and is therefore defined as absolutely stable; this regime suppresses cloud growth. Another effect of the difference between the lapse rates above the mixed layer in WRF and LES is that the temperature is clearly lower in the region between 2 and 3 km height for LES compared to WRF. Therefore a parcel with a similar temperature could rise much higher in this layer in LES compared to WRF, because its buoyancy remains positive at higher altitude.

Both the conditionally unstable layer in LES and the absolutely stable layer in WRF above the inversion are also seen at 14 LT and 17 LT. It is remarkable that, despite the equivalent initial profiles, WRF and LES shows a clearly different profile between 2000 and 3000 m later on during the day.

By analysing the LES results in terms of cloud formation, we find that shallow cumuli have developed already, with their base around 900 m and top around 1200 m. On the first sight, this corresponds with the cloud layer that we can expect from the LES profile, assuming similar adiabat lapse rates as WRF. Instead, the adiabats indicate that a cloud layer is still absent in WRF, and a distinct inversion layer already appears around 1200 m. The temperature increases about 2 K within only 200 m. Notice that a temperature inversion will complicate the onset and vertical development of clouds, so it can be a significant reason for the absence of a cloud layer.

At 14 LT, the well-mixed layer has developed to the level of 1700 m in the case of WRF and to 900 m in the case of LES. The temperature of the mixed layer has also increased: temperature is now around 307 K for WRF and 308 K for LES. The specific humidity is about 16 g kg^{-1} for both models.

The inversion layer in WRF is positioned around 1700m. A temperature difference from about 3 K and a drying-out from 15 to 9 g kg^{-1} exists between the mixed layer and the troposphere, so the inversion -which negatively affects shallow cumulus formation- has been developed further. LES shows a small capping inversion, which is vertically extended between 1100, and 1600 m. The inversion is less sharp and less strong than the inversion in WRF; there is only a temperature difference of about 2.5 K over 500 m. The specific humidity does even not show an inversion, rather a transition between the well-mixed layer -with constant q with height- and the cloud layer -decreasing q with height.

If we concentrate on the dry and moist adiabats, we find that a parcel starting with the WRF surface values would ascend up to 1200 m until it saturates. There it potentially can form clouds, up to 1600 m where the parcel again becomes cooler than the environment. So a possible cloud layer could be formed between 1200 and 1600 m. The cloud base according LES is around 1100 m, which is slightly lower than according to WRF. If we use the same adiabatic lapse rate as WRF, we expect a cloud layer extending up to 2500 m altitude. This corresponds with the model results from LES: the

depth of the cloud layer is much greater than in WRF, with the cloud top around 2550 m, reaching a depth of more than 1.5 km. Indeed, it can be seen, as just described, that the cloud overshoots into the stable region above.

At 17 LT, the WRF mixed layer is about 2 K cooler and 1 g kg^{-1} moister than LES mixed layer. Moreover, the temperature inversion from WRF appears to be less strong, which would indicate better conditions for cloud formation. On the other hand, in terms of humidity, we see an extreme dry-out of the layer above the cloud layer. The specific humidity decreases quickly from 15 g kg^{-1} at 1700 m to 3 g kg^{-1} at 2100 m. The specific humidity profile of LES does not show this sharp inversion; the humidity is decreasing slowly with height throughout the whole cloud layer. We see that due to the lack of moisture, the cloud layer developing in WRF is shallow. The adiabats show that a cloud layer exists between 1300 m and 1800 m. Intuitively, this cloud layer again corresponds with the cloud layer that could be constructed using the adiabatic profiles. The cloud base height agrees well with LES, but again we can see that LES clouds are more vertically developed (up to 2800 m).

It is interesting to discuss our results from WRF with the results obtained in the single column model intercomparison study done by LE04. In this respect, we focus on a SCM with a similar cumulus parameterisation scheme as used in this study. MESO-NH (Lafore et al., 1997, Sánchez and Cuxart, 2004) also uses Kain-Fritsch to parameterise convection and will therefore be used as a reference model. Note that these SCM's are provided with 40 levels in the lowest 4 km, so vertical resolution is comparable with the model used in this study.

- (a) MESO-NH results show an average mixed layer temperature of 304 K at 11:30 LT and 306.5 K at 15:30 LT, which is a lower temperature compared to our results and the results from LES, especially in the morning. However, it compares very well with the other SCM's and the KNMI-LES model shown in LE04.
- (b) q_T profiles compare well to results shown here, with average mixed layer value around 16 g kg^{-1} at 11:30 LT and 16.5 g kg^{-1} at 15:30 LT. Note that MESO-NH shows the q profile which is most similar to the KNMI-LES model of all SCM's shown in LE04.
- (c) General boundary layer structure from MESO-NH is very comparable to LES in the morning (mixed layer height at 800 m; similar lapse rates), as well as in the afternoon (mixed layer height 1200 m, similar lapse rates). It shows a conditionally unstable layer, in contrast to other models, which create a distinct inversion layer, similar as WRF (particularly HIRLAM, but also ECMWF and ECHAM4). This can be linked with the mass flux behaviour of the cumulus parameterisation schemes.

Due to the large scatter in the results shown by LE04, it is clear that parameterisation schemes largely affect the boundary layer structure. In this respect, cloud development is also influenced by the parameterisation schemes. Furthermore, the results from MESO-NH indicate that Kain-Fritsch shows good performance regarding boundary layer characteristics. In the next section, more emphasis will be put on cloud representation in WRF.

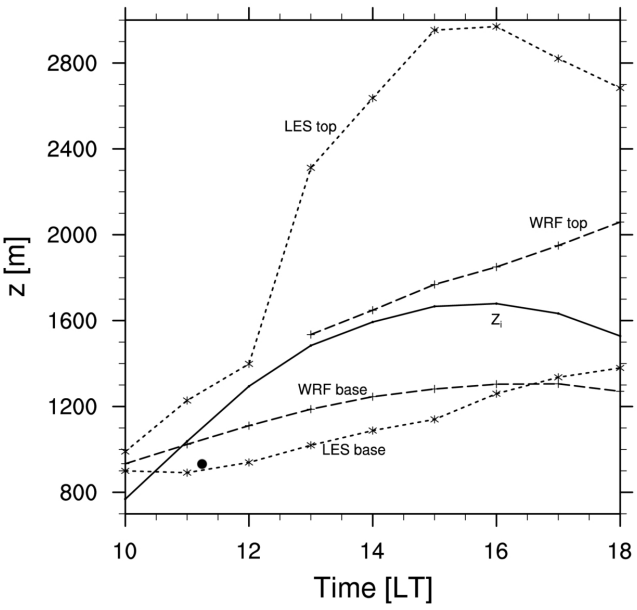

Figure 4. Time evolution of cloud base and top calculated with WRF and based on LES results. Note that in the case of WRF, cloud base is here defined as the LCL. The BL height calculated by WRF, using the Richardson number method, is also given (Z_i, continuous line). The time and LCL height where the mixed layer model came to saturation is indicated with a black dot.

3.3 Cloud Properties

Apart from the analysis of the thermodynamic profiles, we emphasise the properties of the shallow cumulus clouds in LES and WRF. In the previous section we have introduced the theoretical background in order to analyse the clouds. We start with the further analysis of the conditions for shallow cumulus mentioned in the previous section, in order to analyse the cloud properties we can extract from the theoretical behaviour. Next we compare this theory with the actual cloud properties that we can extract from the model results.

A necessary condition for shallow cumulus formation is that a lifting condensation level should be below the boundary layer height (condition (a)); if the humidity conditions are such that air parcels get saturated before their ascent is limited by a capping inversion, clouds may develop. Figure 4 shows the cloud base and top from LES and WRF, together with the boundary layer height calculated by WRF. We assume that the boundary layer height for both models have comparable values during the early morning. As mentioned earlier, cloud base and LCL have equivalent

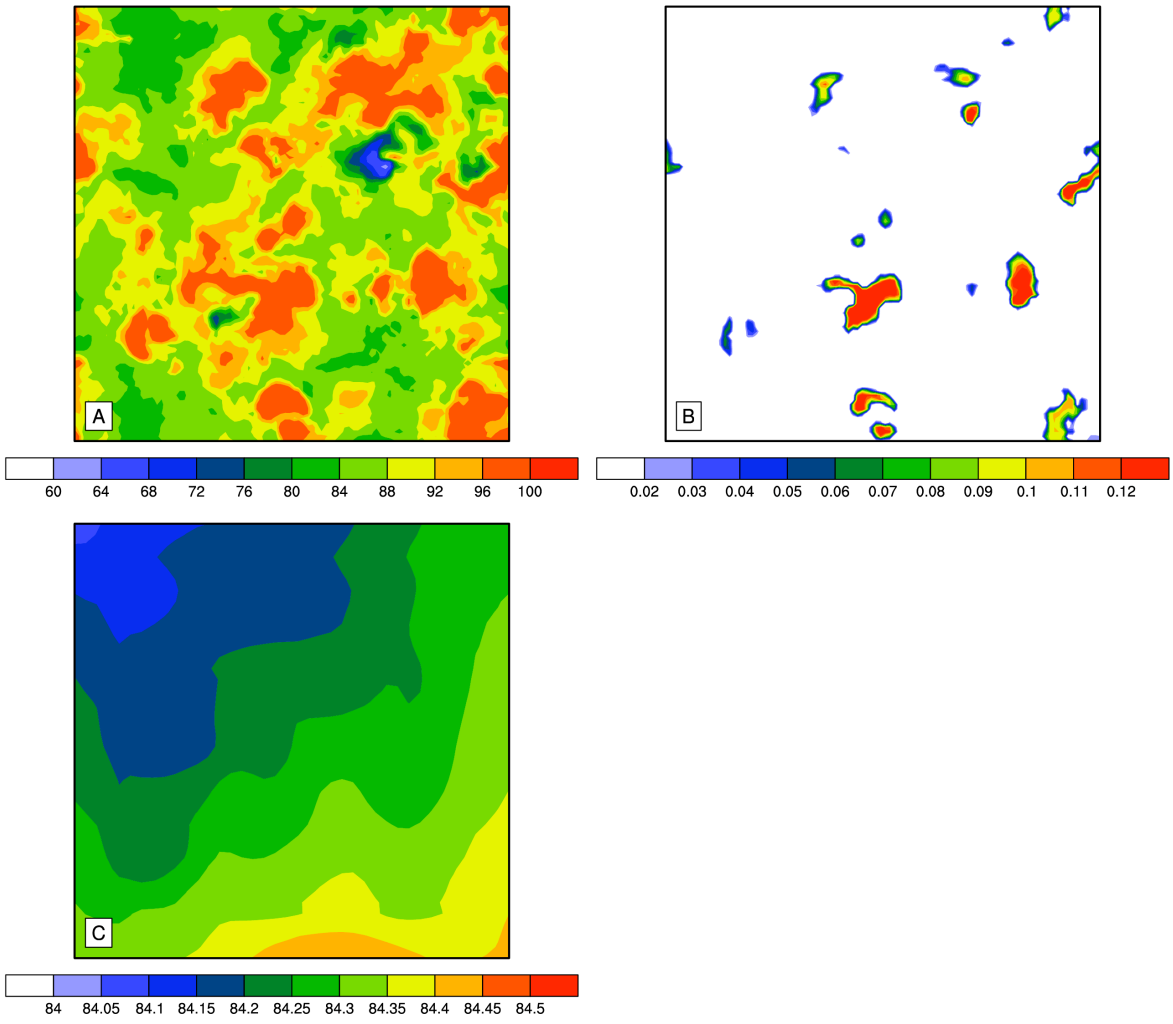

Figure 5. Horizontal cross section of the relative humidity (%) at 14 LT for LES (A) and WRF (C) near the height of the LCL (approximately 1060 m, see Figure 3). The cloud liquid water cross section (g kg^{-1}) for LES has also been plotted (B). For details see text. Note that the areas shown in this Figure have different constraints: A and B is the LES domain (6.4 x 6.4 km^2) and C represents the third domain of WRF (41 x 41 km^2).

heights. If we apply the condition LCL$<Z_i$, clouds could potentially form around 10:30 LT for a LCL around 900 m for LES and around 11 LT with LCL around 1000 m for WRF. A mixed layer model simulation (Tennekes, 1973) has also been performed, which is based on simple parcel theory and uses the same condition LCL$<Z_i$ to identify the start of cloud formation. Moreover, the same surface forcing as shown in Figure 2 are used. Based on its results, cloud formation would start around 11:30 LT at a height of 920 m. The considerable similarity in the results indicate that, based on typical conditions for shallow cumulus conditions, we would expect shallow cumulus formation starting around 10 - 11 LT.

Additionally, we focus on the daily evolution of the cloud depth. Note that the LES cloud base and top shown in Figure 4 have been calculated by the model itself, while the WRF cloud base and top are based on the thermodynamic analysis shown in the previous subsection. Note that in the case of LES, the results of the determination of the height of the cloud base and top between the analysis by means of the parcel method and the model results show large similarities. If we concentrate on WRF first, one can see that the clouds start to form only around 13 LT. The difference between the predicted onset time by the LCL$<Z_i$ condition could be a consequence of either the idea that this condition is not or only partly able to predict the onset time properly, or by an inefficient working of the model itself or the parameterisation scheme.

However, it is clear that this condition is satisfied in the case of LES; the predicted cloud onset of 10:30 LT compares well with the starting time of cloud formation by the model itself, around 10 LT (see Figure 4). Therefore, we conclude

Table 2. The predicted time of onset of clouds (LT), according to different methods discussed in this study. For details, see text.

Model	Parcel method	LCL$<Z_i$	Model - cloud liquid water
LES	10 LT	10:30 LT	10 LT
WRF	13 LT	11 LT	Never

that the cloud representation in WRF can only be caused by unrealistic calculations by the model itself.

Concentrating on the LES cloud depth -remember that this is a model result- we see that the clouds start at 10 LT and grow rapidly during the morning, reaching a maximum depth at 12 LT of about 2 km. As mentioned briefly in the analysis of the thermodynamic profiles, this LES model cloud depth result is very similar to the cloud depth we could expect from the adiabatic profiles in Figure 3.

Most of Single Column Models from LE04 let cloud condensation start around 10 LT, which is comparable to the result from the LES model; however, results are largely scattered in the onset and amount of clouds, depending on cloud scheme and convection and turbulence calculations (LE04). MESO-NH (with Kain-Fritsch CPS) shows a very realistic cloud fraction, fluctuating from 20 to 60% during the day, but too little cloud liquid water compared to LES. This again corresponds to the mass flux behaviour, which is too active transporting heat and moisture from subcloud to cloud layer (see Section 3.5).

Summarizing, we can notice that LES (and thus observations), the mixed layer model and most of the SCM's show that the condition LCL$<Z_i$ is satisfied during 21st June 1997. The analysis of thermodynamic analysis gives additional evidence of the onset and vertical development of these clouds. Based on this analysis, we expect also WRF to represent a cloud layer, although it is expected to develop later on in the day and to be shallower compared to LES.

We have obtained comparable surface forcing (a), a reasonable boundary layer structure, analysed by the parcel method (b) and realistic cloud characteristics derived from theory (c) in WRF compared to LES. Apart from this, the question arises if WRF reproduces the shallow cumulus in terms of the formation of cloud liquid water. In this respect, the model results from WRF are in contrast with the results described in sections a-c. As a summary, Table 2 gives the predicted onset of clouds according to the parcel method (Section 3.2), the condition LCL$<Z_i$ (Section 3.3) and the model results in terms of the formation of cloud liquid water. It is clear that in the case of LES, the results coincide, but not in the case of WRF. WRF does not calculate any cloud liquid water anywhere during the day, which indicates that the conditions for water vapour condensation are not satisfied. An explanation for this result is difficult to find, because it remains unclear whether it is caused by the fact that the thermodynamic profiles which are provided to WRF do not satisfy the conditions for real cloud formation, or WRF is not able to represent shallow cumulus over land, even by thermodynamic conditions which correspond to a typical shallow cumulus boundary layer. On the other hand, the analysis above has shown the formation of a cloud layer in WRF, which is not represented by the model itself.

The difference of representation of shallow cumulus in LES and WRF can be explained by means of the differences in resolutions and physical assumptions. Due to difference in grid scales between LES and WRF, LES is able to treat cumulus convection as an explicit process within a grid box. It has no cloud scheme, as it calculates cloud liquid water directly out of temperature and humidity. In the case of a mesoscale model like WRF, with large grid scales, none of the grids reach saturation, because shallow cumulus is a sub-grid effect, which cannot cause a larger grid box to condense. In order to further investigate this issue, Figure 5 shows the horizontal cross section of relative humidity at the LCL for both models.

At first, one can see that the average value is comparable, around 89% for LES and 84% for WRF. However, as seen in the figure, the horizontal variation is much greater in LES compared to WRF. The relative humidity fluctuates between 62% and 100% within the domain, while it is almost constant in WRF around 84.2%. As mentioned, the LES resolves the large-scale turbulent motions. In this way it is able to represent vertical motions that are induced by thermals. Consequently some grid cells can represent a thermal and will therefore produce a large relative humidity. In case of relative humidity of 100%, condensation occurs and cloud liquid water will be formed, which can be seen in Figure 5. On the other hand, the WRF grid scale does not permit small-scale thermals to be calculated directly; in contrast to LES, turbulence is parameterised. Because of this and the homogeneous surface conditions, there is very little difference between the relative humidity values between different grid cells.

More evidence of the effect of different physical parameterisations on the calculation of relative humidity is given by the SCM results in LE04. Note that SCM results in LE04 show great scatter in case of maximum relative humidity; its values are estimated around 90 - 98% at 11:30 LT and 85 - 100% at 15:30 LT.

The results described above indicate that WRF is able to represent shallow cumulus convection in terms of the surface turbulent fluxes, the boundary layer structure and the cloud properties. On the other hand, the microphysical representation of shallow cumulus in WRF is poor, due to the sub-grid scale of this phenomenon.

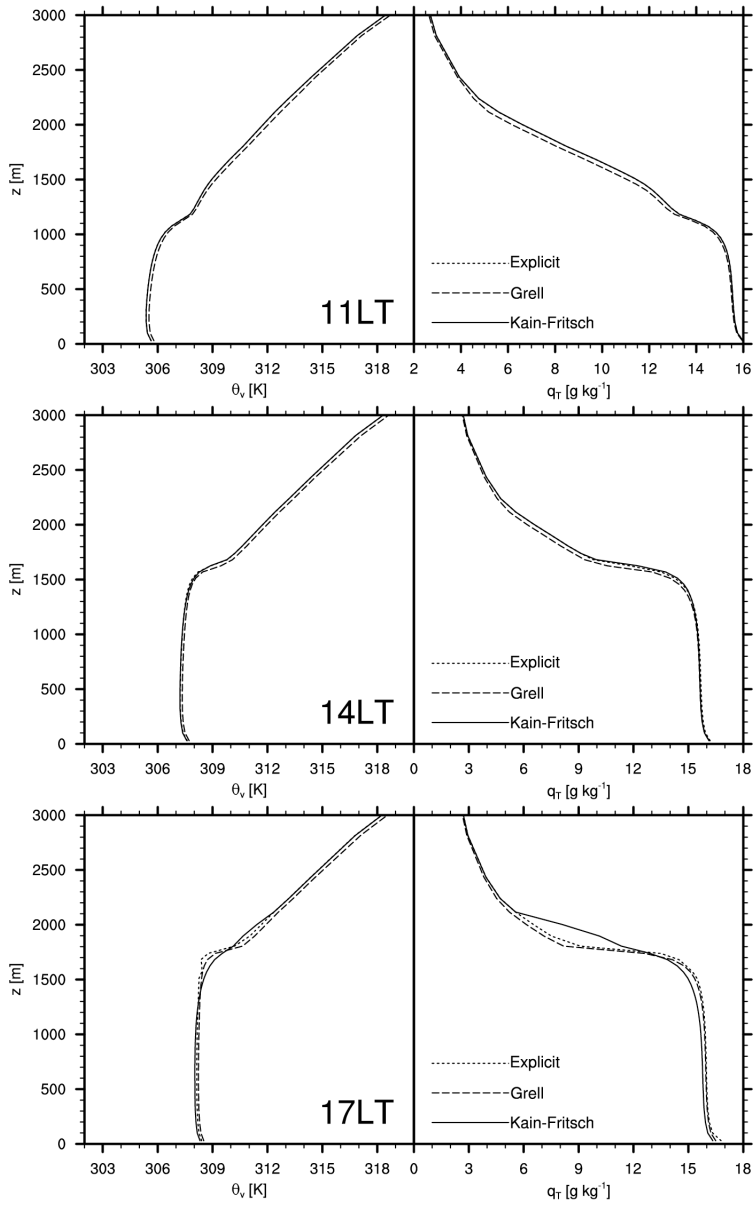

Figure 6. Similar to Figure 3, but in this Figure the vertical profiles of the WRF simulation with the Kain-Fritsch parameterisation scheme (solid), the Grell parameterisation scheme (dashed) and without a parameterisation scheme (dotted) are plotted. Note that the LES results and the adiabats are not included.

3.4 Convective Parameterisation

As discussed before, shallow cumulus convection is sub-grid scale effect and therefore requires a parameterisation to account for this process in mesoscale models. In the previous section we mentioned that the cumulus parameterisation schemes developed by Kain and Fritsch (KF) and Grell (Grell) have shown the best performance with high-resolution models. In this study, we have compared both schemes. In order to complete the comparison, we have done an additional simulation without a CPS. In this simulation (called "explicit"), cloud formation is not parameterised, but calculated directly by the model.

Figure 6 shows the vertical thermodynamic profiles of the WRF simulations with (Kain-Fritsch and Grell) and without a parameterisation scheme. One can see that the profiles show comparable structure at 11 LT and 14 LT. Only at 17 LT, the inversion is much sharper in the explicit simulation and for Grell, both for temperature and humidity, compared to the simulation with Kain-Fritsch. The temperature increases rapidly from 308 K to 311 K at 1700 to 1800 m. In these profiles, the top of the boundary layer is characterised by a thin

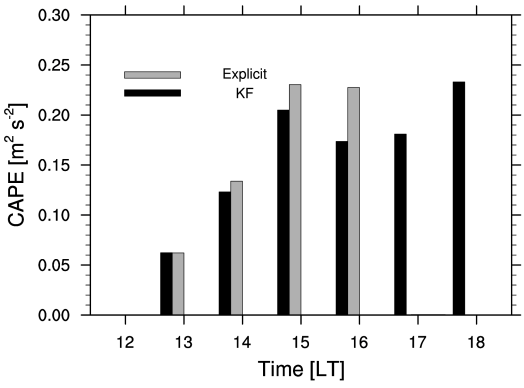

Figure 7. Time evolution of convective available potential energy (CAPE) for WRF simulation with the Kain-Fritsch parameterisation scheme (black) and the simulation without parameterisation scheme (grey).

cloud layer at around 1800 m, which is radiatively cooled at the top. The Grell scheme suggests that WRF temperature and humidity profiles can potentially cause stratiform clouds to form, because of the clear inversion layer. KF, on the other hand, indicates a possible formation of shallow cumulus, but finally does not come up with any cloud signal, as described in detail in the previous subsection. It seems that the conditions for cloud formation are satisfied, but, depending on the parameters within the cumulus scheme, the scheme either shows a different type of cloud, or facilitates shallow cumulus formation, but still finishes without condensation, because some extra conditions within the shallow cumulus scheme are not satisfied. Apparently, Grell favours the condensation over the whole domain, while Kain-Fritsch favours the vertical transport but does not trigger formation of cloud liquid water. This can somehow be related to the findings of Liang et al. (2004), who found that the Grell scheme responds mainly to large-scale vertical motions, while Kain-Fritsch is influenced by near-surface forcing, like in this case.

We have chosen to concentrate on the KF scheme, because, although no clouds are formed, it shows the most realistic behaviour in terms of the dynamic representation of the boundary layer. Note that some single-column models in LE04 also show stratiform boundary layer clouds (HIRLAM) or a large overestimation of cloud liquid water (ECMWF, ARPEGE, ECHAM4), so this appears to be a well-known issue. Apparently, the feedback between cloud formation and microphysics is strongly dependent on the exact formulation of the parameterisation schemes. For all simulations, we have used the Kessler (Kessler, 1969) microphysics scheme. Short test simulations indicated that treating microphysics explicitly did not improve the results.

The CAPE evolution from a shallow cumulus cloud layer is expected to show slow fluctuations in time, because it is a steady phenomenon, which starts in the morning, grows slowly during the afternoon and dies out as soon as the surface fluxes are too small to provide energy input to the boundary layer. Neggers et al. (2004) show the CAPE evolution of the LES simulation. Although the definition of CAPE is slightly different, the daily evolution can be used as a reference to compare with our results shown in Figure 7. The CAPE shows a gradual increase in the morning and afternoon, reaching a maximum at 18 LT and decreasing rapidly to zero in one hour. Therefore, it is clear that the simulation of KF shows the largest correspondence with typical shallow cumulus in terms of the time evolution of the strength of the cloud layer.

To extend this analysis, we can compare the CAPE of the simulation with and without a parameterisation scheme. In this respect, Figure 7 shows the time evolution of CAPE of the cloud layers for both simulations. This Figure shows that the CAPE values from KF simulation are relatively constant in time, increasing from 0.05 to 0.2 m^2 s^{-2} from 13 LT to 15 LT and remaining constant around 0.2 m^2 s^{-2} afterwards. According to the explicit simulation, the CAPE increases strongly during the afternoon from 0.05 to 0.25 m^2 s^{-2} and decreases to zero after 16 LT.

Since KF is the scheme that better reproduces the shallow cumulus convection, we decided to analyse further its performance. As mentioned in Section 2, the KF CPS has a trigger function to account for large-scale vertical motions. We have figured out that the working of the trigger function is not important in this case. Switching it on or off does not change any result. Apparently, an extra temperature boost does not have an effect on the convection type (deep or shallow) under the current conditions. Probably, it can influence the strength of the convection; because if the parcel temperature excess is greater, its buoyancy is larger so potential clouds could be enhanced in their vertical growth. This contradicts with earlier work from Kain and Fritsch (1992) and Jacob and Siebesma (2003), which clearly state that the trigger function is an essential part of the convection scheme; this is possibly only valid for more severe deep convection. LE04 notices that the trigger function is of minor importance in this case, because the shallow convection over land is triggered by surface forcing, not by large scale forcing, represented by a trigger function.

Before the convection parameterisation in KF is activated, several conditions must be satisfied (Kain, 2004). We have classified all updraft source layers (USL) according to these conditions. Firstly, the cloud top height should not be one vertical model level above the height of the LCL. In this way, clouds that are too thin will be removed for further treatment. During the calculation process, about 80% of all USL's are rejected for entrance to the convection routine, because this condition has not been satisfied. Apparently, the LCL's calculated by the scheme, which are based on an empirical relation with the dew point temperature, are clearly overestimated, compared to the results obtained by thermodynamic analysis in this study. We have found that the minimum height of the LCL, calculated by Kain-Fritsch is around 1300 m during the day, while LES and WRF show minimum

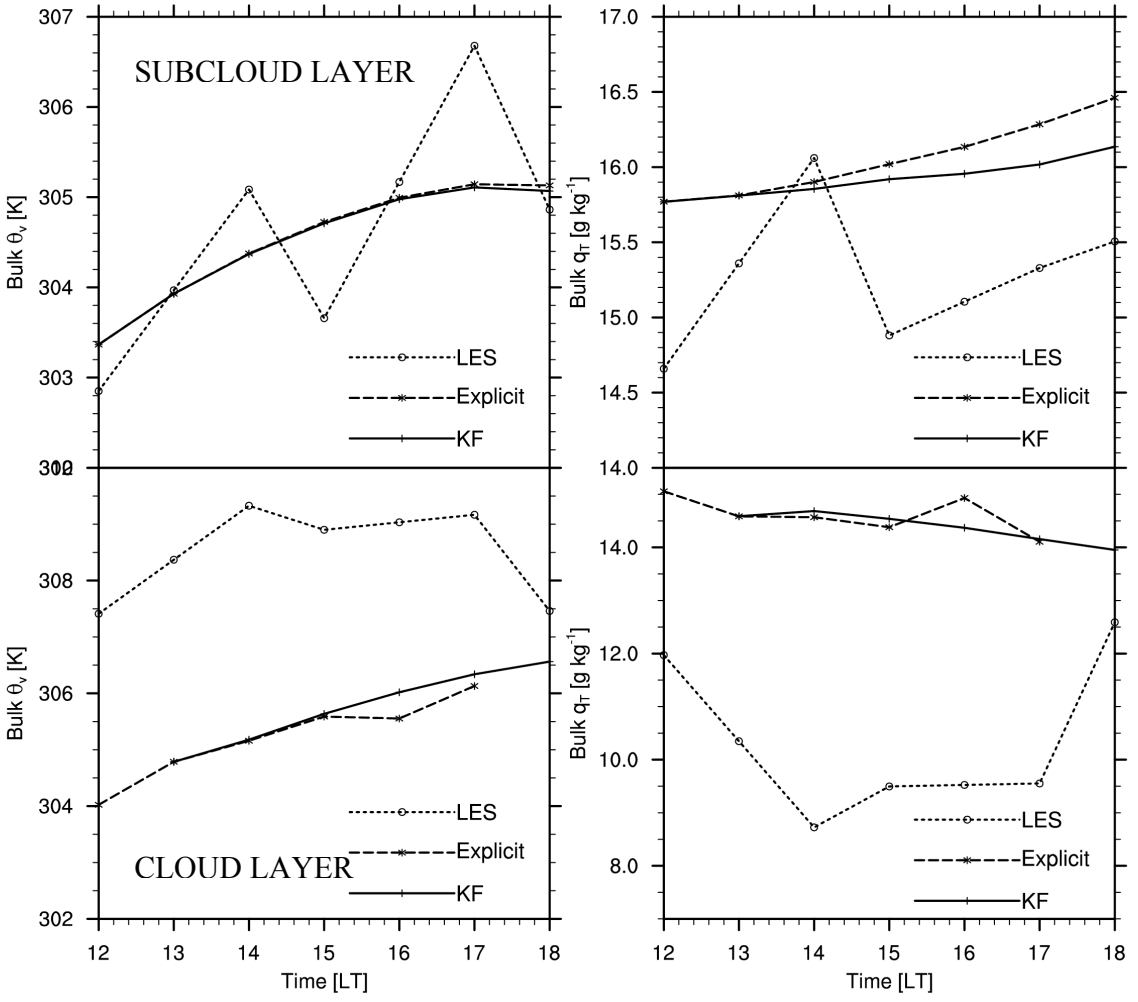

Figure 8. Time evolution of a bulk average of virtual potential temperature (above) and total specific humidity (below) of the subcloud and cloud layer, from WRF with explicit cumulus calculations (solid) and including KF cumulus parameterisation scheme (dashed). The values are averages of the smallest domain.

LCL heights around 900 m (see Figure 5). It remains unclear why: it is hard to compare both LCL heights, as they are based on different calculations; our LCL calculation is based on surface values, while in KF, for each vertical level, which is a candidate for updraft source layer, the LCL is calculated. Another 6% of possible updraft source layers are rejected because the cloud top is located within the boundary layer. Finally, only 13% of all updraft source layers that have started the first calculations remain at this stage.

In the second stage, the cumulus parameterisation scheme identifies the possibility of deep or shallow convection. This selection depends on the following conditions: whether the scheme chooses deep or shallow convection, is determined by the depth of the cloud layer (see above) and the amount of buoyant available energy. All updraft source layers are rejected for deep convection, because the cloud depth never exceeds 2 km, which accords with the results from LES and WRF in Figure 5. As a result, the remaining USL's are used as input in the KF shallow cumulus scheme. Results show that the first USL in Kain-Fritsch is found around 13:50 LT. This agrees encouragingly well with the results of the analysis of the thermodynamic profiles, in which we have determined the start of cloud formation in WRF around 13 LT (see Figures 4 and 5). Besides, the calculations in Kain-Fritsch are based on the identification of different levels; we suspect that an increase of vertical resolution in the model could improve the determination of these levels. Indeed, by defining twice the amount of vertical levels in the boundary layer, we note that first USL's were found more that one hour earlier (12:40 LT), which corresponds better with the results from the analysis with the parcel method.

We can also analyse the behaviour of the scheme by discussing the representation of the dynamical behaviour of shallow cumulus. In this respect, we know that a shallow cumulus enhances the vertical transport of heat and moisture from the subcloud layer into the cloud layer. These layers

are derived from the parcel method analysis from the average profiles shown above and defined as the layer below and above the LCL (see Figure 4). In theory, the parameterisation scheme should be able to represent this sub-grid scale enhanced transport. In order to discuss this issue, we define the vertically averaged values of temperature and moisture of the subcloud layer and the cloud layer. From a theoretical perspective, a shallow cumulus transports heat and moisture from the subcloud layer to the cloud layer, which increases the energy available for cloud formation (LE04). Figure 8 shows the bulk averages for both layers, represented by the WRF simulation with Kain-Fritsch scheme and without a parameterisation scheme. LES results are used as a reference, because they have shown to correspond to typical shallow cumulus boundary layer structure. We see that the virtual potential temperature of the subcloud layer increases during the day from about 303 K to more than 305 K and the total specific humidity of the subcloud layer increases from 15.75 g kg^{-1} to almost 16.5 g kg^{-1} in the explicit simulation and 16.15 g kg^{-1} in the simulation with Kain-Fritsch. The temperature of the subcloud layer is slightly lower (maximum 0.1 K) and the specific humidity higher (0.4 g kg^{-1}) in the case of the simulation with Kain-Fritsch in comparison with the simulation without a parameterisation scheme. Note that the temperature and humidity of the LES simulation are fluctuating significantly in time. Especially in the case of temperature it is not clear if the subcloud layer is warmer or colder for the LES compared to WRF. The temperature and humidity of the cloud layer also show a diurnal evolution. The temperature increases throughout the day from 304 to 306.5 K and the humidity decreases from 15 g kg^{-1} to 14 g kg^{-1}. The differences between the simulations of the cloud layer are less significant but also in this case we can see that the cloud layer is clearly warmer (maximum 0.5 K) and mostly moister (maximum 0.2 g kg^{-1}; except at 16 LT), according to the simulation with Kain-Fritsch, which corresponds to the vertical transport, as discussed before. Although the differences are relatively small, they can be significant enough to enhance sub-grid scale cloud formation. The LES results show a cloud layer with other characteristics than WRF, because this layer is much deeper in this model.

4 Conclusions

This research has investigated how shallow convection over land is represented by the mesoscale model WRF. The case has been based on an idealisation of observations taken at the Atmospheric Radiation Measurement site in Oklahoma, U.S., on 21st June 1997 characterised by the shallow cumulus presence driven by surface forcing with a strong diurnal variation. WRF results are evaluated with large-eddy simulations using very similar surface forcing. The analysis has emphasised the thermodynamic structure of the boundary layer and the cloud properties. Moreover, the results are compared with earlier studies based on single column models. In addition, we study the dependence of shallow cumulus on the variability of surface properties by defining multiple single columns in WRF. The prescribed vertical profiles represent ideal preconditions for shallow convection.

In WRF, the surface turbulent fluxes are calculated assuming a coupling between the land and the atmosphere. In this respect, we have tuned different parameters in order to obtain similar diurnal flux evolution as the one prescribed by LES.

First results indicate that WRF is able to represent the boundary layer structure relatively well. In particular, mixed layer temperature and humidity profiles agree satisfactorily well with LES results. The analysis has been extended to study the vertical temperature profiles of LES and WRF using the parcel method to determine the atmospheric stability at different regions of the boundary layer and the cloud properties. From this, we have concluded that: (a) the inversion in WRF is stronger than the inversion simulated by LES, decreasing the potential for parcels to rise above that inversion; (b) the conditionally unstable lapse rate between 2 and 3 km height, which is a necessary condition for shallow cumulus, is present in LES and absent in WRF; (c) the clouds start to form in the morning for LES and in the morning or early afternoon in WRF, depending on the condition, and reach a maximum depth of 2.5 km for LES and 1 km for WRF.

With respect to the formation of cloud liquid water, we have found that, in contrast to LES, WRF is not producing cloud liquid water. Therefore, it needs to be noted that the differences that were found in the evolution of the boundary layer according to LES and WRF in the analysis with the parcel method can also correspond to the inability of WRF to form cloud liquid water.

Shallow cumulus are characterised by length scales smaller that the typical grid lengths. Consequently, its representation requires the use of parameterisation of the cloud dynamic and physics. In the case under study, we have studied the role of the convective parameterisation in representing the shallow cumulus convection. In this respect, we have shown that the use of a cumulus parameterisation scheme is necessary. Shallow convection parameterisation enhances the vertical transport of heat and moisture from the subcloud layer to the cloud layer. In our study two cumulus parameterisation schemes, Kain-Fritsch and Grell, have been used and compared with the results from an "explicit" simulation. Results from this comparison point out that Kain-Fritsch clearly outperforms Grell and explicit in terms of the representation of the enhanced vertical transport, as well as the vertical structure of the boundary layer. On the other hand, Grell and explicit favour the formation of cloud liquid water which leads to the appearance of a very sharp inversion -which does not correspond to typical conditions of shallow convection. In other words, by using the Grell or explicit physical options the model tends to perform worse. These sensitivity analyses pointed out the strong coupling between cumulus and microphysics parameterisations and

the difficulty in representing the main properties of shallow cumulus in terms of convective transport and liquid water content due to the strong spatial variability within the grid.

References

Bolton, D., 1980: *The computation of equivalent potential temperature*, Mon Wea Rev, **108**, 1046–1053.

Braun, S. A. and Tao, W. K., 2000: *Sensitivity of high-resolution simulations of hurricane Bob (1991) to planetary boundary layer parameterizations*, Mon Wea Rev, **128**, 3941–3961.

Brown, A. R., Cederwall, R. T., Chlond, A., Duynkerke, P. G., Golaz, J. C., Khairoutdinov, M., Lewellen, D. C., Lock, A. P., MacVean, M. K., Moeng, C. H., Neggers, R. A. J., Siebesma, A. P., and Stevens, B., 2002: *Large-eddy simulation of the diurnal cycle of shallow cumulus convection over land*, Quart J Roy Meteor Soc, **128**, 1075–1094.

Buzzi, A., Fantini, M., Malguzzi, P., and Nerozzi, F., 1994: *Validation of a limited area model in cases of mediterranean cyclogenesis: surface fields and precipitation scores*, Meteor Atm Phys, **53**, 137–153.

Callado, A. and Pascual, R., 2005: *Diagnosis and modelling of a summer convective storm over Mediterranean Pyrenees*, Adv Geosci, **2**, 273–277.

de Rooy, W. C. and Siebesma, A. P., 2008: *A simple parameterization for detrainment in shallow cumulus*, Mon Wea Rev, **136**, 560–576.

Ek, M. B. and Holtslag, A. A. M., 2004: *Influence of soil moisture on boundary layer cloud development*, J Hydrometeor, **5**, 86–99.

Fritsch, J. M. and Chappell, C., 1980: *Numerical prediction of convectively driven mesoscale pressure systems. Part I: convective parameterization*, J Atmos Sci, **37**, 1722–1733.

Gochis, D. J., Shuttleworth, W. J., and Yang, Z. L., 2002: *Sensitivity of the modeled North American monsoon regional climate to convective parameterization*, Mon Wea Rev, **130**, 1282–1298.

Grell, G. A., 1993: *Prognostic evaluation of assumptions used by cumulus parameterizations*, Mon Wea Rev, **121**, 764–787.

Grell, G. A. and Devenyi, D., 2002: *A generalized approach to parameterizing convection combining ensemble and data assimilation techniques*, Geoph Res Letters, **29**, 38–1–4.

Grell, G. A., Dudhia, J., and Stauffer, D. R., 1995: A description of the fifth-generation Penn State/NCAR mesoscale model (MM5), NCAR Technical Note, NCAR/TN-398 + STR, 138 p.

Hahmann, A. N., Rostkier-Edelstein, D., Warner, T. T., Liu, Y., Vandenberghe, F., and Swerdlin, S. P., 2008: *Toward a climate downscaling for the Eastern Mediterranean at high-resolution*, Adv Geosci, **12**, 159–164.

Hong, S. Y. and Pan, H. L., 1996: *Nonlocal boundary layer vertical diffusion in a medium-range forecast model*, Mon Wea Rev, **124**, 2322–2339.

Jacob, C. and Siebesma, A. P., 2003: *A new subcloud model for mass-flux convection schemes: influence on triggering, updraft properties and model climate*, Mon Wea Rev, **131**, 2765–2778.

Janjić, Z. I., 1994: *The step-mountain Eta coordinate model: further developments of the convection, viscous sublayer, and turbulence closure Schemes*, Mon Wea Rev, **122**, 927–945.

Jimenez-Guerrero, P., Jorba, O., Baldasano, J. M., and Gasso, S., 2008: *The use of a modelling system as a tool for air quality management: Annual high-resolution simulations and evaluation*, Sci Tot Env, **390**, 323–340.

Kain, J. S., 2004: *The Kain-Fritsch convective parameterization: an update*, J Appl Meteor, **43**, 170–181.

Kain, J. S. and Fritsch, J. M., 1990: *A one-dimensional entraining/detraining plume model and its application in convective parameterization*, J Atmos Sci, **47**, 2784–2802.

Kain, J. S. and Fritsch, J. M., 1992: *The role of convective "trigger function" in numerical forecasts of mesoscale convective systems*, Meteor Atmos Phys, **49**, 93–106.

Kessler, E., 1969: On the distribution and continuity of water substance in atmospheric circulation, Meteorological Monograph vol. 32, American Meteorological Society, 84 p.

Kuo, Y. H., Reed, R. J., and Liu, Y., 1996: *The ERICA IOP 5 storm. Part III: mesoscale cyclogenesis and precipitation parameterization*, Mon Wea Rev, **124**, 1409–1434.

Kuo, Y. H., Bresch, J. F., Cheng, M. D., Kain, J. S., Parsons, D. B., Tao, W. K., and Zhang, D. L., 1997: *Summary of a mini workshop on cumulus parameterization for mesoscale models*, Bull Amer Meteor Soc, **78 (3)**.

Lafore, J. P., Stein, J., Asencio, N., Bougeault, P., Ducrocq, V., Duron, J., Fischer, C., Héreil, P., Mascart, P., Masson, V., Pinty, J. P., Redelsperger, J. L., Richard, E., and Vilà-Guerau de Arellano, J., 1997: *The Meso-NH atmospheric simulation system. Part I: adiabatic formulation and control simulations*, Ann Geoph, **90**, 90–109.

Lenderink, G., Siebesma, A. P., Cheneit, S., Ihrons, S., Jones, C. G., Marquet, P., Muller, F., Olmera, D., Calvo, J., Sánchez, E., and Soares, P. M. M., 2004: *The diurnal cycle of shallow cumulus clouds over land: a single-column model intercomparison study*, Quart J Roy Meteorol Soc, **130**, 3339–3364.

Liang, X. Z., Li, L., Dai, A., and Kunkel, K. E., 2004: *Regional climate model simulation of summer precipitation diurnal cycle over the United States*, Geoph Res Letters, **31**, L24 208.1–L24 208.4.

Moeng, C., 2006: *Towards real-world applications of large-eddy simulations*, Eos Trans AGU, **87 (52)**, Abstract H53F–01.

Neggers, R. A. J., Siebesma, A. P., Lenderink, G., and Holtslag, A. A. M., 2004: *An evaluation of mass flux closures for diurnal cycles of shallow cumulus*, Mon Wea Rev, **132**, 2525–2538.

Neggers, R. A. J., Neelin, J. D., and Stevens, B., 2007: *Impact Mechanisms of Shallow Cumulus Convection on Tropical Climate Dynamics*, J Climate, **20**, 2623–2642.

Petch, J. C., Brown, A. R., and Gray, M. E. B., 2002: *The impact of horizontal resolution on the simulations of convective development over land*, Quart J Roy Meteor Soc, **128**, 2031–2044.

Sánchez, E. and Cuxart, J., 2004: *A buoyancy-based mixing-length proposal for cloudy boundary layers*, Quart J Roy Meteor Soc, **130**, 3385–3404.

Siebesma, A. P., Bretherton, C. S., Brown, A., Chlond, A., Cuxart, J., Duynkerke, P. G., Jiang, H., Khairoutdinov, M., Lewellen, D., Moeng, C. H., Sánchez, E., Stevens, B., and Stevens, D. E., 2003: *A large eddy simulation intercomparison study of shallow cumulus convection*, J Atmos Sci, **60**, 1201–1219.

Skamarock, W. C., Klemp, J. B., Dudhia, J., Gill, D. O., Barker, D. M., Wang, W., and Powers, J. G., 2005: A description of the advanced research WRF version 2, NCAR Technical Note, NCAR/TN-468+STR, 88 p.

Steeneveld, G. J., Mauritsen, T., Bruijn, E. I. F., Vilà-Guerau de Arellano, J., Svensson, G., and Holtslag, A. A. M., 2008: *Evaluation of limited-area models for the representation of the diurnal*

cycle and contrasting nights in CASES-99, J Appl Meteor Climatol, **47**, 869–887.

Stull, R., 1988: An introduction to boundary layer meteorology, Kluwer Academic Publishers, 680 p.

Stull, R., 2000: Meteorology for scientists and engineers, Brooks/Cole, 502 p.

Tennekes, H., 1973: *A model for the dynamics of the inversion above a convective boundary layer*, J Atmos Sci, **30**, 558–567.

Tiedtke, M., 1989: *A comprehensive mass flux scheme for cumulus parameterization in large-scale models*, Mon Wea Rev, **117**, 1779–1800.

Tudurí, E. and Ramis, C., 1997: *The environments of significant convective events in the Western Mediterranean*, Wea Forecasting, **12**, 294–306.

van Heerwaarden, C. C. and Vilà-Guerau de Arellano, J., 2008: *Relative humidity as an indicator for cloud formation over heterogeneous land surfaces*, J Atmos Sci, **65**, 3263–3277.

Vilà-Guerau de Arellano, J., 2007: *Role of nocturnal turbulence and advection in the formation of shallow cumulus over land*, Quart J Roy Meteorol Soc, **133**, 1615–1627.

Wang, W. and Seaman, N. L., 1997: *A comparison study of convective parameterization schemes in a mesoscale model*, Mon Wea Rev, **125**, 252–278.

Zhong, S., In, H., and Clements, C., 2007: *Impact of turbulence, land surface, and radiation parameterizations on simulated boundary layer properties in a coastal environment*, J Geophys Res, **112**, D13 110.1–D13 110.14.

Zhu, P. and Albrecht, B., 2002: *A theoretical and observational analysis on the formation of fair-weather cumuli*, J Atmos Sci, **59**, 1983–2005.

Zhu, P. and Bretherton, C. S., 2004: *A simulation study of shallow moist convection and its impact on the atmospheric boundary layer*, Mon Wea Rev, **132**, 2391–2409.